Supplementary Information

Endothelial-LRP1 clears major amounts of $A\beta_{1-42}$ across the blood-brain barrier

Steffen E. Storck[1], Sabrina Meister[1,*], Julius Nahrath[1,*], Julius N. Meißner[2], Nils Schubert[2], Alessandro Di Spiezio[3], Sandra Baches[4], Roosmarijn E. Vandenbroucke[5,6], Yvonne Bouter[2], Ingrid Prikulis[4], Carsten Korth[4], Sascha Weggen[4], Axel Heimann[7], Markus Schwaninger[3], Thomas A. Bayer[2] and Claus U. Pietrzik[1]

[1]Institute for Pathobiochemistry, University Medical Center of the Johannes Gutenberg-University, Mainz, Germany. [2]Division of Molecular Psychiatry, Department of Psychiatry and Psychotherapy, University Medical Center (UMG), Georg-August-University Goettingen, Goettingen, Germany. [3]Institute of Experimental and Clinical Pharmacology and Toxicology, University of Luebeck, Germany. [4]Department of Neuropathology, Heinrich Heine University Duesseldorf, Germany. [5]Inflammation Research Center, VIB, Ghent, Belgium. [6]Department of Biomedical Molecular Biology, Ghent University, Ghent, Belgium. [7]Institute for Neurosurgical Pathophysiology, University Medical Center of the Johannes Gutenberg-University, Mainz, Germany.

*these authors contributed equally to this work

Correspondence should be addressed to C.U.P. (pietrzik@uni-mainz.de), University Medical Center of the Johannes Gutenberg-University of Mainz, Institute for Pathobiochemistry, Molecular Neurodegeneration, Duesbergweg 6, 55099 Mainz, Germany, phone: +49-6131-39-25390, fax: +49-6131-39-26488, mail: pietrzik@uni-mainz.de

Conflict of interest statement

The authors have declared that no conflict of interest exists.

Supplementary Methods

Tamoxifen injection

To test if tamoxifen injection alters LRP1 expression in brain endothelium, 4-7 week-old wt mice were injected intraperitoneally with 2 mg tamoxifen (T5648, Sigma-Aldrich, Darmstadt, Germany) or ethanol as control for 7 consecutive days. The analysis of LRP1 expression was examined tree days after the last treatment by western blotting of lysates of isolated brain endothelial cells.

Isolation of adult neurons, astrocytes and microglia

Adult neurons, astrocytes and microglia were isolated from the cortex of 12 week old mice according to a protocol published elsewhere (1).

Motor tests

The balance beam, string suspension, and rotarod were performed as described previously (2, 3).

Supplementary Figures

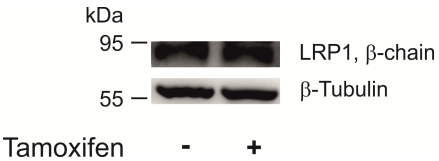

Supplementary Figure 1. **Tamoxifen injection does not alter LRP1 expression in brain endothelial cells.** Wt mice were injected with tamoxifen as described in supplementary methods. Lysates of isolated brain endothelial cells were analyzed via western blotting. Anti-β-tubulin immunoblot is shown as a loading control.

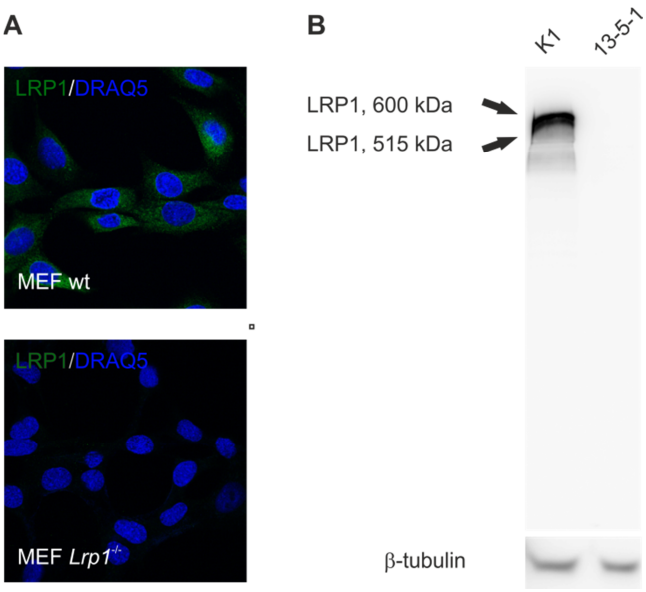

Supplementary Figure 2. Novel monoclonal LRP1-antibody 11E2 binds to LRP1 N-terminus. (A) Immunofluorescent staining of wild-type (wt) and *Lrp1* knockout (*Lrp1*$^{-/-}$) mouse embryonic fibroblast (MEF) cells with 11E2. (B) Western blot analysis of CHO cells (K1) and *Lrp1* knockout (13-5-1) cell lysates with 11E2. Anti-β-tubulin immunoblot is shown as a loading control.

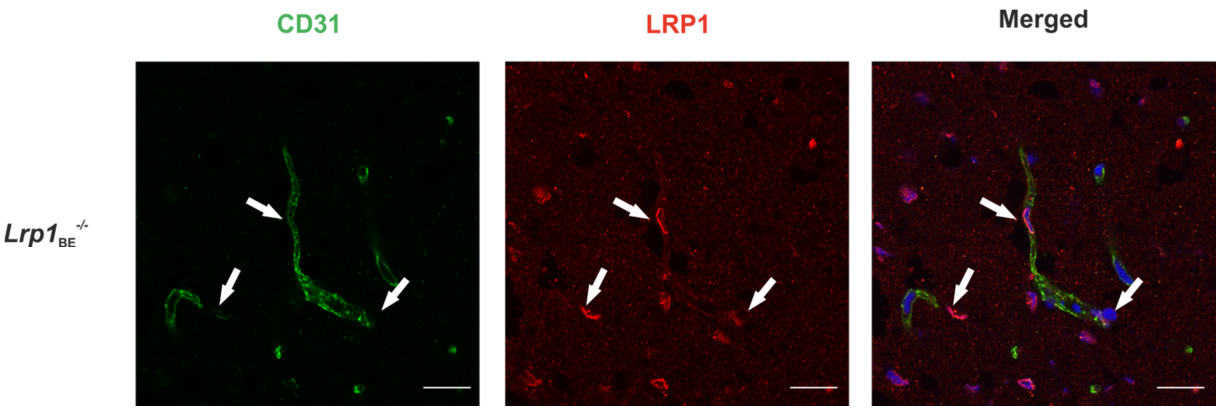

Supplementary Figure 3. CD31-negative cells adjacent to the endothelium are not affected by Cre-recombination in *Lrp1*$_{BE}^{-/-}$ mice. Immunofluorescent staining for endothelial cell marker CD31 and LRP1 show CD31-negative cells adjacent to the endothelium are show LRP1 expression in *Lrp1*$_{BE}^{-/-}$ mice. Scale bar, 20 µm.

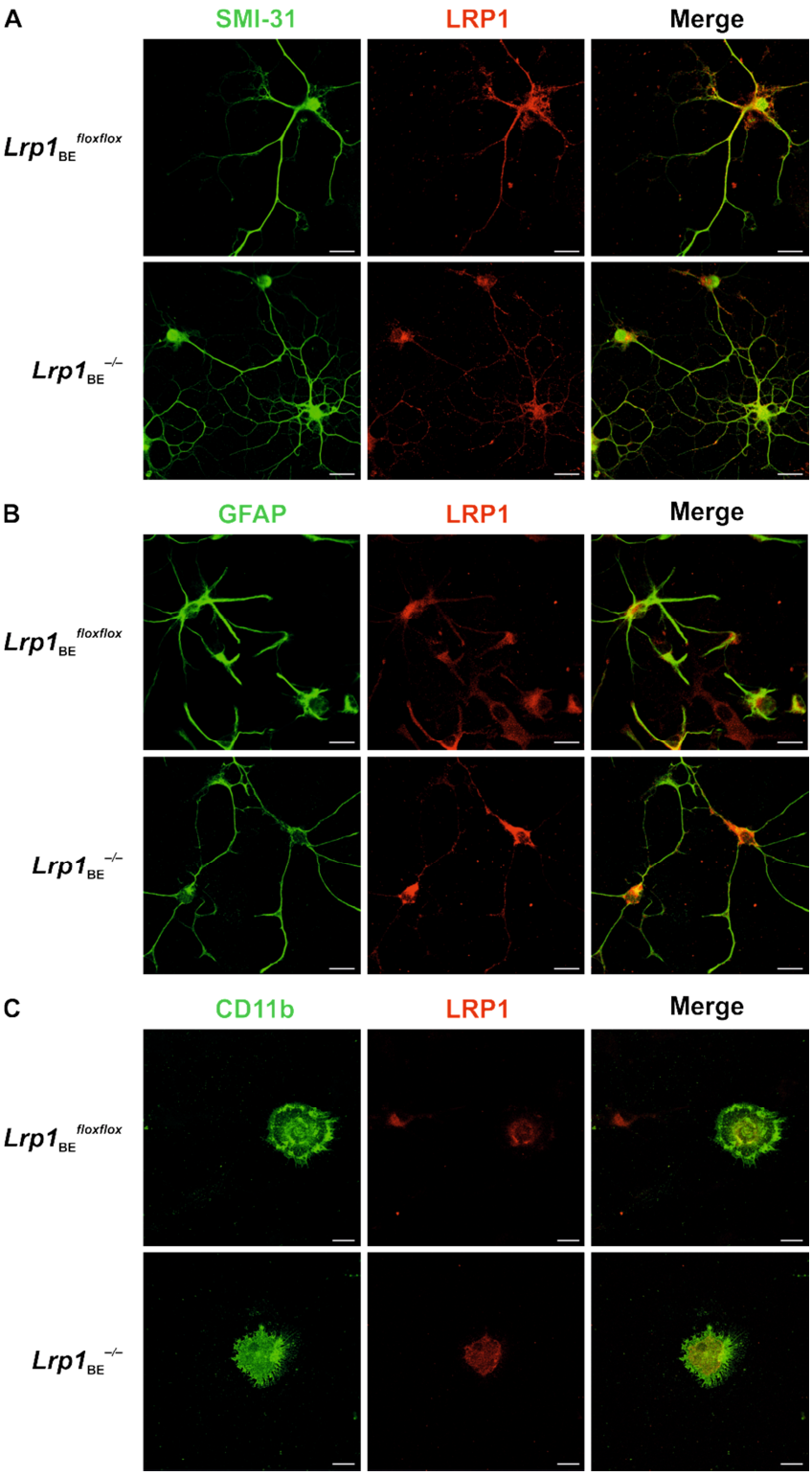

Supplementary Figure 4. LRP1 expression in isolated neurons, astrocytes and microglia of *Lrp1*$_{BE}^{-/-}$ mice. Immunofluorescent staining of isolated primary cells of adult mice for LRP1 and (A) SMI-31-positive neuronal cells, (B) GFAP-positive astrocytes, and (C) CD11b-positive microglia to determine potential recombination in microglia, neurons, and astrocytes revealed no differences between genotypes. Scale bar, 20 µm.

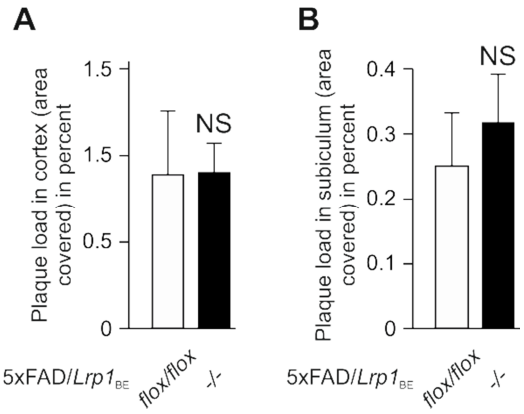

Supplementary Figure 5. No difference in plaque load between 5xFAD/*Lrp1*$_{BE}^{flox/flox}$ and 5xFAD/*Lrp1*$_{BE}^{-/-}$. No effect of brain endothelial-specific knockout on plaque load deposition in (A) cortex and (B) subiculum. Values represent means ± s.e.m. of n=5 (5xFAD/*Lrp1*$_{BE}^{flox/flox}$) and n=4 (5xFAD/*Lrp1*$_{BE}^{-/-}$). For statistical analyses, unpaired t-test was used.

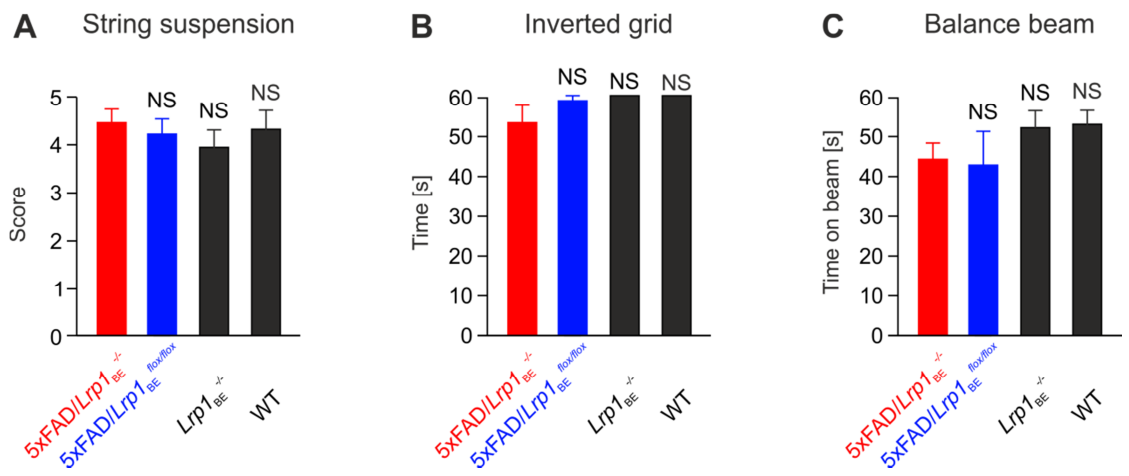

Supplementary Figure 6. No early motor deficits in 5xFAD/*Lrp1*$_{BE}^{-/-}$. Analysis of motor performance revealed no deficits in string suspension (A) the inverted grid (B), and balance beam (C) task in 5xFAD/*Lrp1*$_{BE-/-}$ and 5xFAD/*Lrp1*$_{BE}^{flox/flox}$ mice. Values represents means ± s.e.m. of n=6, n=7, n=4, n=8 from groups left to right.

Supplementary Table 1: Antibodies and dyes used in specific application

Primary Antibody (Catalog #, manufacture, dilution)	**Secondary antibody Catalog #, manufacture, dilution)**	**Application**
1704 rabbit anti-LRP1 (4), (IHC: 1:2000, WB: 1:10000)	Alexa Fluor-546 goat anti-rabbit (A11010, Thermo Fisher Scientific, 1:1000) HRP-conjugated goat anti-rabbit (A5278, Sigma, 1:10000)	Detection of LRP1 in Figure 3A and Supplementary Figure 4A; analysis of LRP1 β-chain in Figures 1B, 2A, Supplementary Figure 1
11E2 mouse anti-LRP1, novel mAb (Supplementary Figure 2), (IHC 5.2 µg/ml, WB: 1:1000)	Alexa Fluor-546 goat anti-mouse (A11018, Thermo Fisher Scientific, 1:1000) HRP-conjugated goat anti-mouse (A9169 Sigma, 1:5000)	Detection of LRP1 in Figures 1A, 3B-C, Supplementary Figure 2A, Supplementary Figure 3 and Supplementary Figure 4B-C; analysis of LRP1 α-chain in 2A and Supplementary Figure 2B
Rabbit anti-β-actin (A2066, Sigma-Aldrich, 1:1000)	HRP-conjugated goat anti-rabbit (A5278, Sigma, 1:10000)	WB control in Figures 1B and 2A
goat anti β-actin (SC-1615, Santa Cruz, 1:2000)	HRP-conjugated rabbit anti-goat (P0160, Dako, 1:2000)	WB analysis control in Figure 4A
Rat anti-CD31 (550274, BD Pharmingen, 1:100)	Alexa Fluor-488 goat anti-rat (A11006, Thermo Fisher Scientific, 1:1000)	Endothelial marker in Figure 1A and Supplementary Figure 3
IC16 mouse anti-Aβ (5) (WB: 1:500)	HRP-conjugated goat anti-mouse (A9169 Sigma, 1:5000)	capture antibody for ELISA of Aβ in Figure 7L and M, Analysis of Aβ in Figure 7A-C
6E10 mouse anti-Aβ (SIG-39320-500, Covance, 4µg/mg beads)		Immunoprecipitation of Aβ in in Figure 7A-C
mouse anti-β-tubulin (Sigma-Aldrich, 1:10000)	HRP-conjugated goat anti-mouse (A9169 Sigma, 1:5000)	WB control in Supplementary Figure 1 and Supplementary Figure 2B
mouse anti-NeuN (MAB377, Merck Millipore, 1:100)	Alexa Fluor-488 goat anti-rat (A11006, Thermo Fisher Scientific, 1:1000)	Neuronal marker in Figure 3A
rabbit anti-GFAP (Z0334, Dako, 1:500)	Alexa Fluor-546 goat anti-rabbit (A11010, Thermo Fisher Scientific, 1:1000)	Astrocyte marker in Figure 3B and Supplementary Figure 4B
rat anti-CD11b 1:100 (Serotec),	Alexa Fluor-488 goat anti-rat (A11006, Thermo Fisher Scientific, 1:1000)	Marker for microglia and macrophages in Figure 3C and Supplementary Figure 4C
mouse anti-SMI31 (SMI-31R, Sternberger, 1:1000)	Alexa Fluor-488 goat anti-rat (A11006, Thermo Fisher Scientific, 1:1000)	Neuronal marker in Supplementary Figure 4A
rabbit anti-GFAP (173002, Synaptic Systems, 1:1000)	Biotin-conjugated swine anti-rabbit (E0353, Dako, 1:200)	Detection of activated astrocytes in Figure 8B
Rabbit anti-IBA1 (019-19741, Wako, 1:1000)	Biotin-conjugated swine anti-rabbit (E0353, Dako, 1:200)	Detection of activated microglia in Figure 8A
Draq5 (DR50200, Biostatus Limited, 5 µM)		Nuclei staining in Figures 1, 3, Supplementary Figure 2A and Supplementary Figure 3

Supplementary References

1. Brewer GJ, and Torricelli JR. Isolation and culture of adult neurons and neurospheres. *Nat Protoc.* 2007;2(6):1490-8.
2. Jawhar S, Trawicka A, Jenneckens C, Bayer TA, and Wirths O. Motor deficits, neuron loss, and reduced anxiety coinciding with axonal degeneration and intraneuronal Abeta aggregation in the 5XFAD mouse model of Alzheimer's disease. *Neurobiol Aging.* 2012;33(1):196 e29-40.
3. Wirths O, Breyhan H, Schafer S, Roth C, and Bayer TA. Deficits in working memory and motor performance in the APP/PS1ki mouse model for Alzheimer's disease. *Neurobiol Aging.* 2008;29(6):891-901.
4. Pietrzik CU, Busse T, Merriam DE, Weggen S, and Koo EH. The cytoplasmic domain of the LDL receptor-related protein regulates multiple steps in APP processing. *EMBO J.* 2002;21(21):5691-700.
5. Jager S, Leuchtenberger S, Martin A, Czirr E, Wesselowski J, Dieckmann M, Waldron E, Korth C, Koo EH, Heneka M, et al. alpha-secretase mediated conversion of the amyloid precursor protein derived membrane stub C99 to C83 limits Abeta generation. *J Neurochem.* 2009;111(6):1369-82.